IS-T-694

TEMPERATURE DEPENDENCE OF RESISTIVITY OF THIN FILM SAMPLES OF CHALCOGENIDE GLASSES

Anand Krishnarao Kulkarni

M. S. Thesis Submitted to Iowa State University

Ames Laboratory, ERDA
Iowa State University
Ames, Iowa 50011

Date Transmitted: October 1975

PREPARED FOR THE U. S. ENERGY RESEARCH AND DEVELOPMENT ADMINISTRATION UNDER CONTRACT NO. W-7405-eng-82

DISCLAIMER

Available from: National Technical Information Service
U. S. Department of Commerce
P.O. Box 1553
Springfield, VA 22161

Price: Microfiche $2.25

Temperature dependence of resistivity of thin film samples of chalcogenide glasses

by

Anand Krishnarao Kulkarni

A Thesis Submitted to the
Graduate Faculty in Partial Fulfillment of
The Requirements for the Degree of
MASTER OF SCIENCE

Department: Physics
Major: Solid State Physics

Approved:


In Charge of Major Work


For the Major Department


For the Graduate College

Iowa State University
Ames, Iowa

1975

TABLE OF CONTENTS

LIST OF TABLES

LIST OF FIGURES

1. INTRODUCTION

The chalcogenide glasses have become a matter of great concern in recent years because of their potential use as switching and memory devices.[1-3] Research on the multicomponent chalcogenide glasses was spurred by the discovery that most of them have ordinary semiconducting electrical properties with a room temperature conductivity of the order of $10^{-9}\ \Omega^{-1}\ cm^{-1}$. Amorphous Tl_2Se-As_2Te_3, however, has a room temperature conductivity of $10^{-3}\ \Omega^{-1}\ cm^{-1}$ which is larger than the conductivity of many crystalline semiconductors.[4]

Multicomponent chalcogenide glasses are essentially covalent in nature and are remarkably insensitive to accidental impurities. They contain a large number of unsaturated chemical bonds capable of engaging and satisfying the valence requirements of any impurity. This factor and the possibility of internal rearrangements without lattice constraints are believed to preclude the impurities from acting as donors or acceptors of electrons as they would in crystalline semiconductors. In this sense, at least, such glasses must be regarded as almost intrinsic semiconductors.

It is extremely difficult to determine the structure of multicomponent chalcogenide glasses by means of x-ray or electron diffraction experiments. However, the amorphous nature can be verified by noting the absence of Bragg scattering peaks. Structural investigations by x-ray diffraction due to Hilton et al.[5] on a bulk sample of $Ge_{15}As_{45}Te_{40}$ glass yield a radial distribution function with two

peaks at 2.50 and 4.02 Å. The position of the first peak corresponds to an average of all interatomic distances which range from 2.43 Å (Ge-Ge) to 2.86 Å (Te-Te). A nuclear magnetic resonance study[6] of amorphous and crystallized $Te_{81}Ge_{15}As_4$ showed a 0.1% chemical shift of the Te peak from that of the crystalline Te.

For a large class of multicomponent chalcogenide glasses, the electrical conductivity increases exponentially with increasing temperature in accordance with the ordinary semiconductor expression

$$\sigma = \sigma_0 e^{-E_\sigma/kT}$$

with σ_0 between $10^2\,\Omega^{-1}\,cm^{-1}$ and $10^4\,\Omega^{-1}\,cm^{-1}$ and the activation energy E_σ in the 0.3 to 1.0 eV range.[7,8] Quinn and Johnson[9] have measured the electrical conductivity of a bulk sample of $Ge_{15}Te_{80}As_5$ in the temperature range 230-330 K. The values of E_σ and σ_0 obtained by them are 0.43-0.48 eV and $(1\text{-}5) \times 10^3\,\Omega^{-1}\,cm^{-1}$, respectively. The values of resistivities on TeAsGeS glasses obtained by Mackowski et al.[10] lie in the range of 10^4 to $10^6\,\Omega cm$. Their results also show an increase in resistivity with an increase in percentage of Ge in the glass. The room temperature resistivity and activation energy have been measured for four different samples in the form of bulk and evaporated films of As-Te-Ge by R. Pinto.[11] My own research group members have measured temperature dependence of resistivity of bulk samples of $As_{15}Te_{73}Ge_{12}$ and $As_{15}Te_{70}Ge_{15}$ and have reported the activation energies of 0.37 eV and 0.30 eV and σ_0 values of $50\,\Omega^{-1}\,cm^{-1}$ and $5\,\Omega^{-1}\,cm^{-1}$

respectively. Bunton et al.[12] measured the resistivity and activation energy of Ge-Te-As-Si samples in the form of bulk, evaporated films and sputtered films, and have come to the conclusion that the resistivities and activation energies of sputtered films had values which were closer to the corresponding values for the bulk material rather than to the values for evaporated films. Hence it was decided to measure the resistivities and activation energies of the As-Te-Ge thin film samples prepared by RF sputtering.

Measurements of the Seebeck coefficients have been performed on several multicomponent chalcogenide glasses, and it is generally agreed that p-type conduction predominates in this class of materials. Seager et al.[13] have measured both Hall coefficients and Seebeck coefficients in As_{50}-Te_{45}-Ge_5 and As_5-Te_{80}-Ge_{15} samples. The Hall coefficients indicated n-type conduction and an activation energy E_H of 0.06-0.07 eV. E_H is the activation energy obtained from Hall coefficients. The room-temperature value of the Hall mobility, μ_H = 0.053 cm^2/V-sec, obtained by Panus et al.[14] is in good agreement with the results of Seager et al. But the Seebeck coefficients for the same samples showed p-type conductivity and their data gave an activation energy E_s = 0.24 eV and 0.29 eV for $As_5Te_{80}Ge_{15}$ and $As_{50}Te_{45}Ge_5$ respectively. E_s is the activation energy obtained from Seebeck coefficients. The conductivity measurements on the same samples yield activation energies E_σ = 0.43 eV and 0.46 eV for the $As_5Te_{80}Ge_{15}$ and $As_{50}Te_{45}Ge_5$ glasses respectively. E_σ is the activation energy obtained from conductivity measurements.

Rockstad[15] has measured the ac conductivity of $Te_{48}As_{30}Si_{12}Ge_{10}$ and he has observed that the ac conductivity equals the d.c. conductivity up to 10^4 to 10^5 Hz, but the ac conductivity increases with frequency approximately proportional to $\omega^{0.9}$ in the 10^5 to 10^8 Hz region.

Optical absorption spectra of chalcogenide glasses always exhibit relatively sharp absorption edges, from which optical gaps can be deduced.[7,8] It appears that thin films of a given composition absorb light of all frequencies to a somewhat greater extent than do bulk samples of the same composition, but the position of the optical edge is the same within experimental error.[16] Thus the exponential dependence of electrical conductivity over a wide temperature range and the reasonably distinct wavelength limits in the absorption spectra strongly support the view that multicomponent chalcogenide glasses may be regarded as intrinsic semiconductors.

II. APPARATUS

Figure 1 shows the entire apparatus which consists of a resistance measuring unit, a temperature control unit and a temperature measuring unit.

A. Resistance Measuring Circuit

For the measurement of high resistances an apparatus built by Mr. Robert Johnson[17] in 1966 has been used. The block diagram of the apparatus is shown in Fig. 2. It is claimed that this instrument can measure sample impedances as high as 10^{15} to 10^{16} ohms. In the measuring circuit the current supply provided a voltage varying from 0 to 10 volts across the sample. The current was determined by measuring the voltage across a variable resistor. In most cases, because of the high resistance of the samples, a resistance of 100.1 MΩ has been used to obtain readable voltages across the variable resistor. This voltage was measured by a Keithley model 601 electrometer which has a maximum sensitivity of 1 mV full scale with input impedance of 10^{14} Ω.

The voltage across the sample was measured by the null method using battery operated potentiometers and Victoreen model 475 BR dynamic capacitor electrometers functioning as null indicators. After 30 minutes warm up, it was necessary to calibrate the potentiometer P_3 by the 601 electrometer. In order to read the voltage across the variable resistor accurately a digital Hewlett-Packard RMS voltmeter (3403 A) was connected to the 601 electrometer.

THIS PAGE

WAS INTENTIONALLY

LEFT BLANK

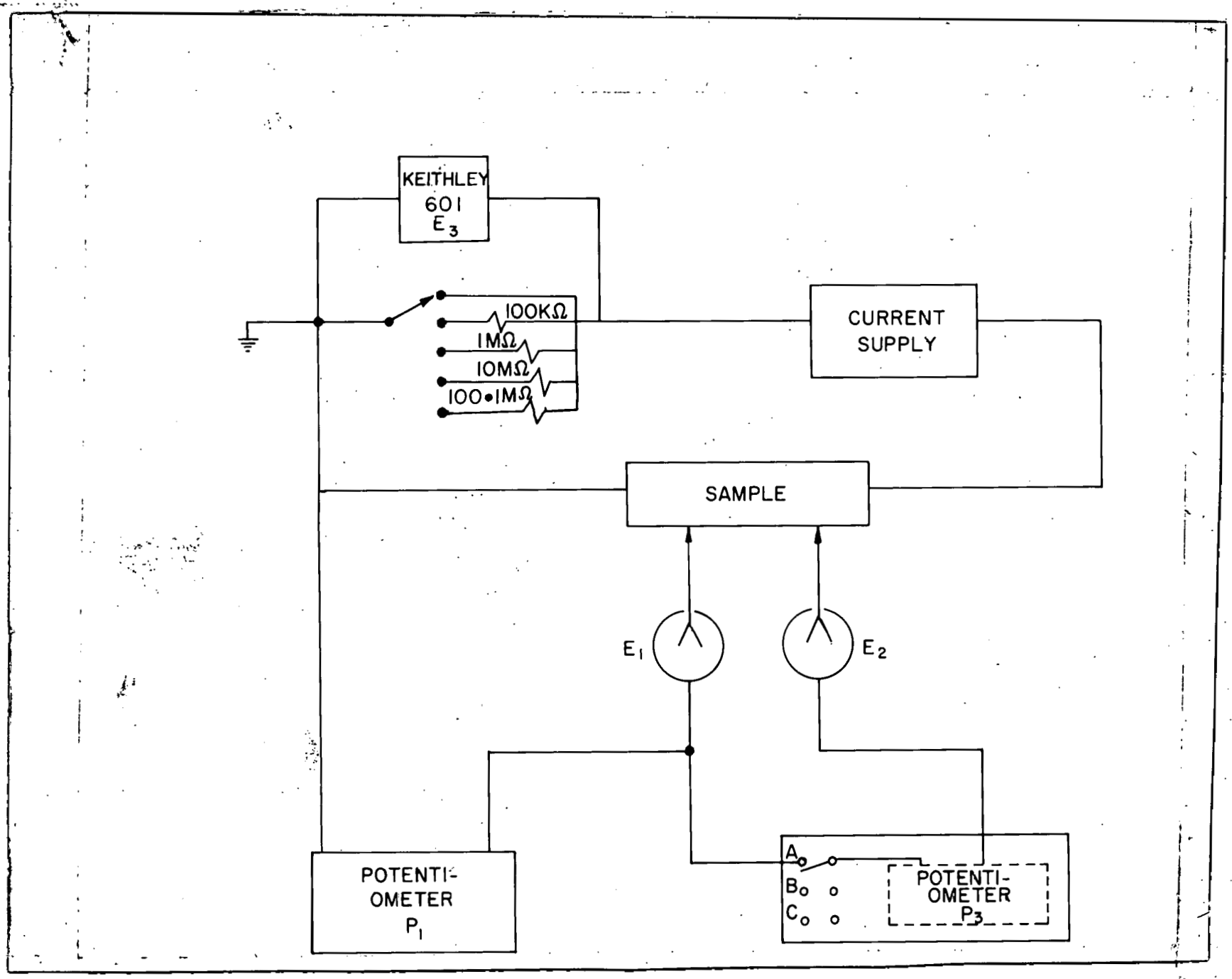

Fig. 2. Block diagram of the resistance measuring circuit.

B. Sample Holder

The sample holder is shown in Fig. 3 and Fig. 4. The important parts are the following.

(1) A hollow copper disc forms the base of the system through which cold water can be passed to maintain the temperature of the sample fairly constant. This copper disc also serves as a heat sink for the thermo-electric cooler which is mounted on top of it.

(2) A standard Borg-Warner thermo-electric cooler (0.5" x 0.5") (Model 094492) is used to vary the temperature of the sample from -30° C to +30° C. This thermo-electric cooler was mounted on the copper disc using tin-indium eutectic solder. While soldering, proper care was taken not to heat the thermo-electric cooler excessively (limit is 125° C). Number 18 copper wires, which were covered with teflon coating, were leads to the thermo-electric cooler.

(3) On top of the thermo-electric cooler a copper plate of thickness 1/32" is soldered with indium.

(4) Epoxy, which has high electrical insulation and good thermal conduction was used to mount the YSI precision thermistor on the copper plate (part #44003). The resistance of the thermistor is 1000 Ω at 25° C, and varies from 10.92 K at -30° C to 833.7 Ω at +30° C. However, because of the glass substrate between copper plate and sample, the actual variation in temperature of the copper plate was much greater than the temperature variation of the sample. The operating temperature range of the thermistor is from -80° C to +150° C. The thermistor leads are #28 manganin wires with teflon

THIS PAGE

WAS INTENTIONALLY

LEFT BLANK

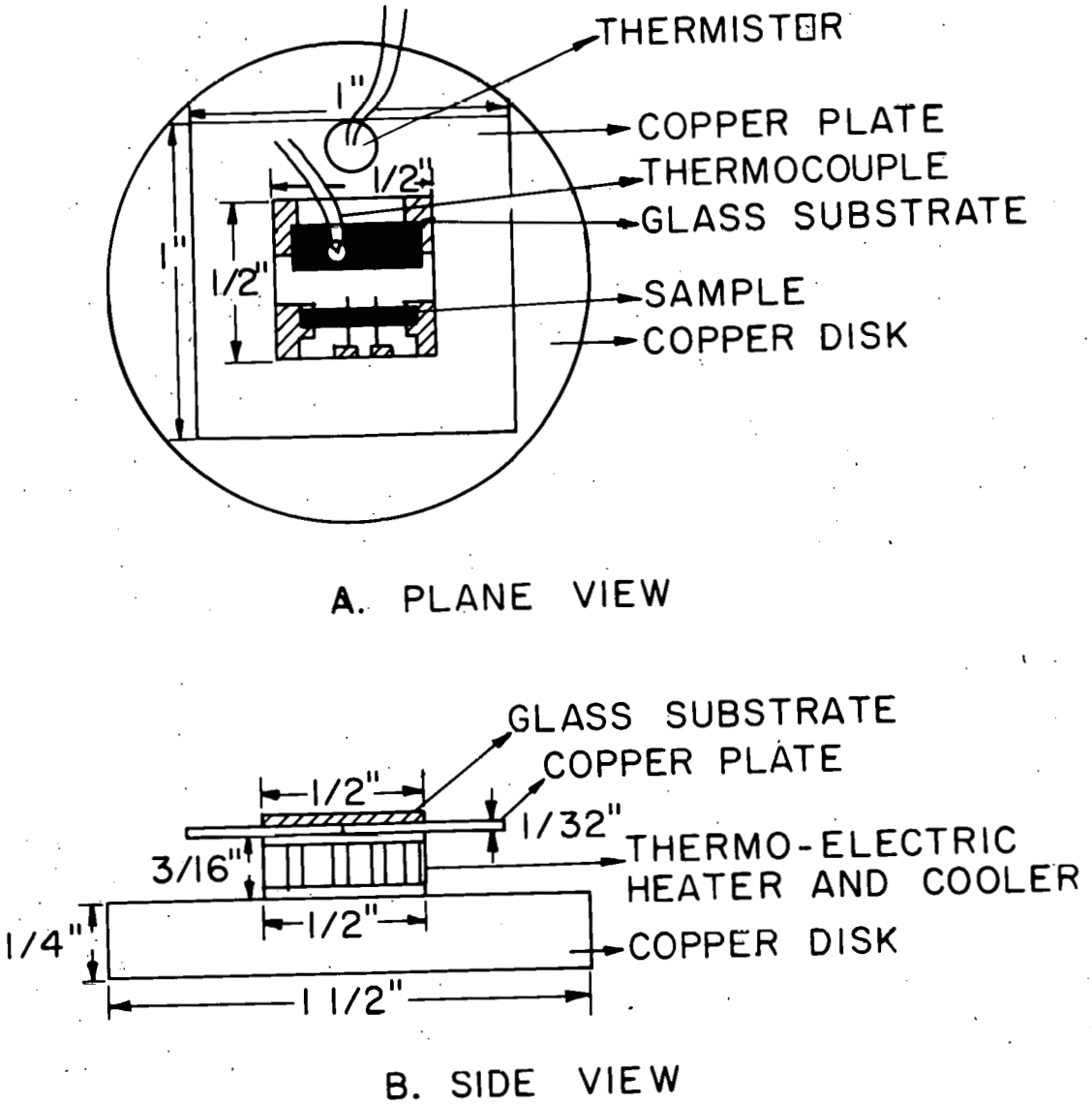

Fig. 4. Schematic diagram showing the details of the sample holder.

coating. One must take extra precaution in handling the thermistor leads since they are likely to break at the joints if they are twisted.

(5) The current and voltage probes are made of thin copper plate. These probes are clamped to the copper plate with teflon screws. Teflon pieces having sufficient thickness were placed between the probes and copper plate to achieve high electrical insulation. Again #28 manganin wire was used for connections. The substrate holder is tightly held on the copper plate by the current and voltage probes. Sufficient care was taken, while tightening the screws, not to impose heavy mechanical stress on the thermo-electric cooler.

(6) A copper-constantan thermocouple was mounted on the sample that had been sputtered specially for such purposes. Indium solder made a good contact between the thermocouple and sample.

C. Temperature Control and Power Supply

The circuit diagram for the temperature control and power supply is shown in Fig. 5. In the power supply unit a transformer converted 110 V a.c. to 6.3 V a.c. with 10 amperes current. This voltage was rectified by a bridge circuit using 12 F 10 diodes. A filter circuit of an inductor (0.01 H) and a capacitor (4000 μF, 25 V) was used to obtain ripple free d.c. It was possible to obtain 0 to 10 V.d.c. by adjusting the variable transformer. An Eltex modular power supply was connected directly across 110 V a.c. to obtain +15 and -15 V for the operational amplifiers in the temperature control unit.

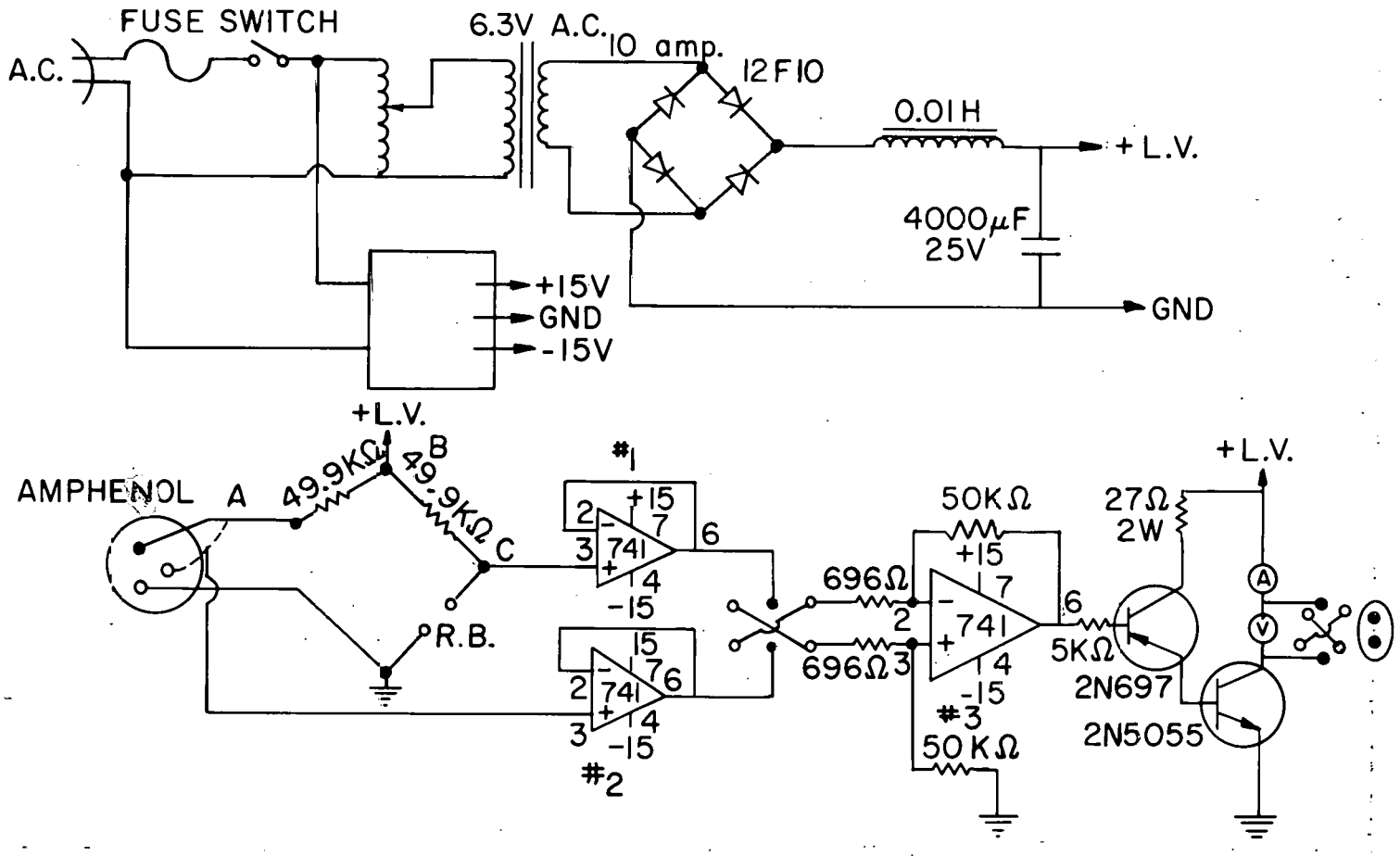

Fig. 5. Circuit diagram for temperature control and power supply. On top is the circuit diagram of power supply and on bottom is the circuit diagram for temperature control.

In the temperature control unit, two 49.9 kΩ one percent resistors formed two arms of the Wheatstone bridge. The third and fourth arms of the bridge were a thermistor (1000 Ω at 25° C) mounted on top of the copper plate in the sample holder, (Fig. 5) and a Rubicon Company resistance box (1 Ω to 10,000 Ω in steps) respectively. If the bridge was unbalanced by choosing a resistance (> 1000 Ω) from the resistance box, a difference in the potential resulted across the bridge (A and C). This differential potential was fed to the 741 operational amplifiers (#1 and #2) which were mainly used to obtain a low output impedance from a high input impedance. The third 741 operational amplifier magnified the input difference potential about 100 times to drive the transistor 2N697 which in turn drove the transistor 2N5055. A gradual increase in the voltage and current was observed in the voltmeter and current meter respectively. The switch passed the current through the thermo-electric cooler in a particular direction to cool the sample. This cooling of the sample cooled the thermistor as well, and the resistance of the thermistor increased. The difference in potential across the bridge decreased and the voltmeter and ammeter indicated a decrease in the voltage and current respectively. This process continued until the thermistor resistance was almost equal to the resistance of the resistance box. The bridge was almost balanced and the current in the thermo-electric cooler was just sufficient to maintain the sample at the required temperature. Thus it was possible to decrease the sample temperature to a minimum of -30° C by taking the highest resistance from the

resistance box. On the other hand by choosing a resistance (< 1000 Ω) it was possible to pass current through the thermo-electric cooler in the opposite direction to heat the sample. A temperature of +30° C could be obtained by decreasing the resistance to 100 Ω in the resistance box. The rate of heating and cooling was also dependent on the low voltage (L.V.) obtained from the power supply. By choosing a particular resistance from the resistance box and adjusting the variable transformer in the power supply it was possible to obtain any desired temperature of the sample in the temperature range -30° C to +30° C. A copper-constantan thermocouple was used as a temperature sensor, and the EMF of the thermocouple was measured by a type K-3 universal potentiometer.

III. SAMPLE PREPARATION

RF sputtering is a very useful technique to obtain amorphous thin films of multicomponent samples.[18] The main target of $Te_{75}As_{25}$ prepared by Dr. B. F. T. Bolker, one of our group members, has been used to obtain films of high Te content. The target was fabricated from 99.9999% purity Te and As. As shown in Fig. 6 the subtargets [0.04 cm (1/64 in.) thick slices of semiconductor grade Ge] rested on top of the Te-As main target and were held in place by gravity. The four slices were of different sizes and placed to give the desired Ge content to the films.

The substrates were standard 1.3 cm x 1.3 cm x 0.08 cm. Corning 7059 glass plates with typical surface smoothness of 1/2 micro inch. Contact pads of Mo of thickness 7000 Å were previously sputtered on these substrates. To insure good thermal contact with the holder, the substrates were coated on the backside with Ga-In eutectic. Five individual substrates were used to obtain different compositions of Ge as shown in Fig. 6.

With the aid of an aluminum mask, rectangular-shaped [0.85 cm x 0.15 cm] films of As-Te-Ge of thickness 1-2 μm have been sputtered between the contact pads (Fig. 4). Another rectangular-shaped film was sputtered to make thickness measurements. The first and second run of samples were made without bias. The third run of samples was sputtered under 20% bias.

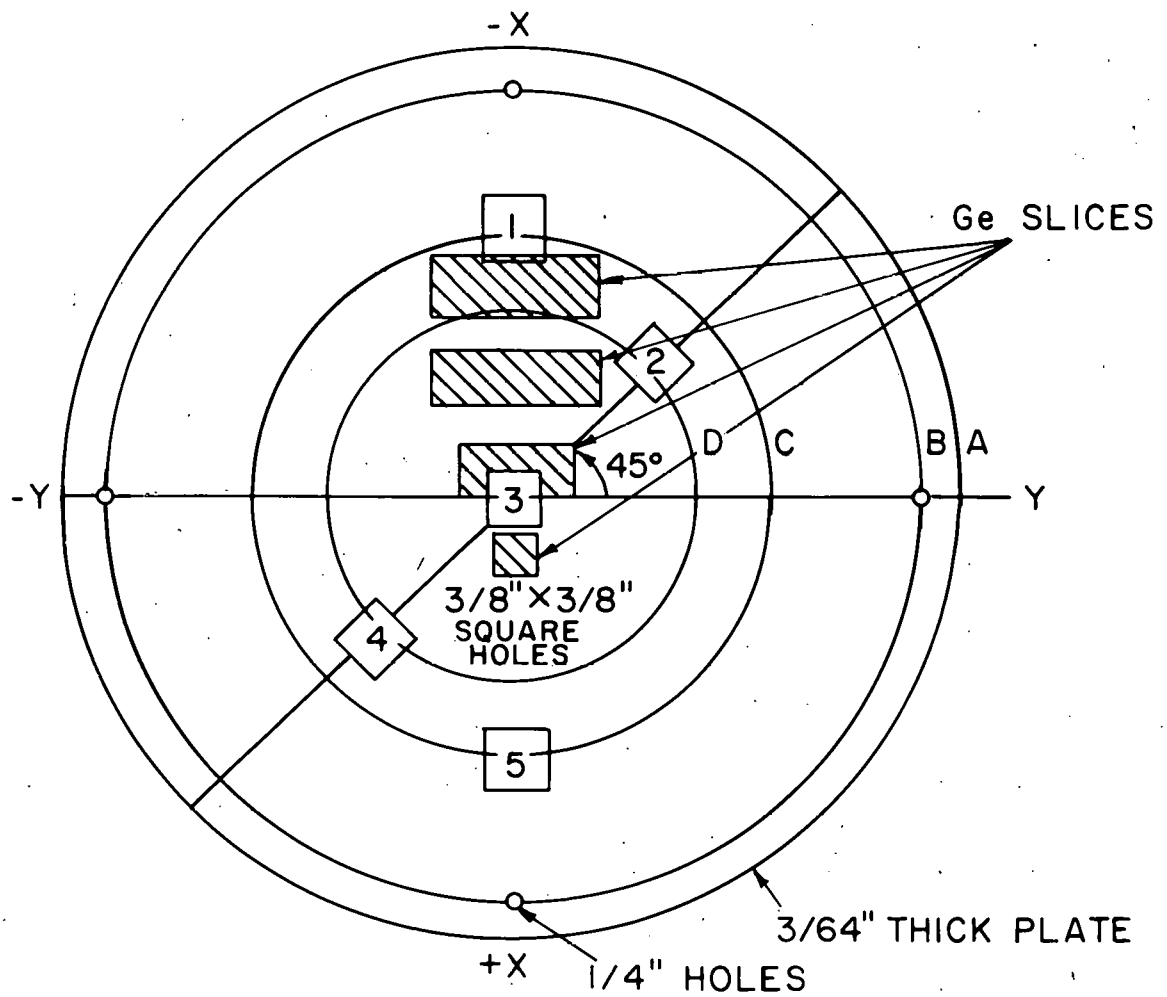

DIMENSIONS:

RADIUS OF CIRCLE A = 3"
" " " B = 2 11/16"
" " " C = 1 3/4"
" " " D = 1 5/16"

DISTANCE BETWEEN TARGET AND SUBSTRATE = 2.5"

Fig. 6. Schematic diagram of glass substrates and arrangement of Ge slices on $As_{25}Te_{75}$ target.

IV. MEASUREMENTS AND RESULTS

A. Electron Microprobe Analysis

An Applied Research Lab model EMX electron microprobe was used to analyze the samples compositionally for weight percent of the Te, As, and Ge constituents. A standard computer program "Magic IV"[19] converted the microprobe readings to atomic percent of the constituents. The primary beam voltage was 10 KeV which provided a sample current of approximately 43 nA. The counts for all three constituents were detected by L_α spectral line.

Within 100 μm of the center of each sample several microprobe readings were taken. The sample was moved under the electron beam at the rate of 96 microns/minute during the 40 second integration time (counting time) of each measurement. This slow rate prevented sample heating and the possibility of vaporizing the film's constituents. The composition of each film as determined by these individual readings did not vary by more than a few tenths atomic percent. The arithmetic average of these separate measurements was chosen to specify the film's actual composition.

The micro-probe was precalibrated with bulk standards consisting of Te, As, and Ge pieces that came from the same lot of material that was used for the target. The mean depth of beam penetration into the film was 0.4 μm. Since all films were thicker than 1.0 μm, there was no problem with the electrons penetrating the substrate. The absolute accuracy of these analyses was $\pm$ 2%[19] which includes instrumental errors,

standardization errors and small vibrations in beam locations on the film.

It is possible to analyze the composition of the samples theoretically from known deposition profiles and from film thickness measurements by the use of the superposition equation[20]

$$T(P_0) = t \sum_{j=1}^{N} G_j(P_0) R_j(0') \qquad (1)$$

where $T(P_0)$ is the total film thickness at any point $P_0(x_0, y_0)$ of the planar substrate, t is the sputtering time, $G_j(P_0)$ is the deposition profile, and $R_j(0')$ is the deposition rate at some reference point which is chosen to be the center of the substrate plane $0'(0, 0)$ (Fig. 7). Depending on the geometry of the substrate and subtarget arrangement it is possible to calculate the deposition profile $G(P_0)$. For the case of rectangular co-ordinates illustrated in Fig. 7 the deposition profile is[20]

$$G(P_0) = \int_{y_1}^{y_2} dy \int_{x_1}^{x_2} dx \frac{D^2}{[(x - x_0)^2 + (y - y_0)^2 + D^2]^2} . \qquad (2)$$

The fundamental function for this double integral is

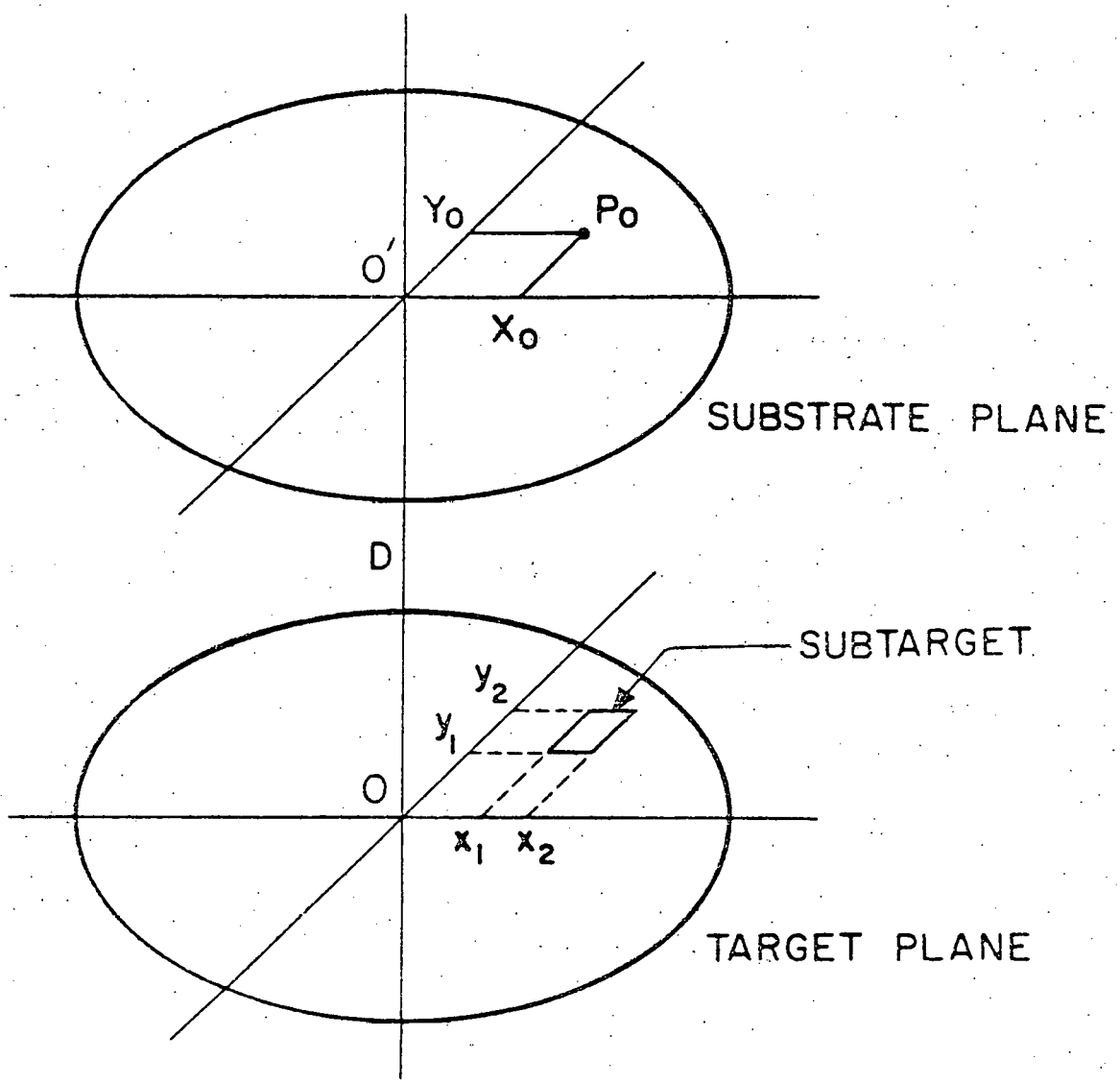

Fig. 7. Cosputtering geometry for rectangular coordinates.

$$F(x, y) = \frac{1}{2}\left\{ \frac{x - x_0}{\sqrt{(x - x_0)^2 + D^2}} \text{ arc tg } \frac{y - y_0}{\sqrt{(x - x_0)^2 + D^2}} \right.$$

$$\left. + \frac{y - y_0}{\sqrt{(y - y_0)^2 + D^2}} \text{ arc tg } \frac{x - x_0}{\sqrt{(y - y_0)^2 + D^2}} \right\}. \qquad (3)$$

Using this fundamental function the deposition profile can be expressed as

$$G(P_0) = \int_{x_1}^{x_2} dx \int_{y_1}^{y_2} dy \frac{\partial^2 F(x,y)}{\partial x \, \partial y} = \{F(x_2, y_2) - F(x_1, y_2)$$

$$- F(x_2, y_1) + F(x_1, y_1)\} \qquad (4)$$

In equations 2, 3 and 4, (x, y) are co-ordinates of the subtarget location, (x_0, y_0) is a point on the substrate, and D is the separation between target and substrate.

The calculated values of $G(P_0)_{Ge}$ for different substrates due to different Ge slices (Fig. 6) are given in Table la. These values of $G(P_0)$ are normalized with respect to the profile for the total composite target area at some fixed point on the substrate such as the origin (0'). Similarly the normalized values of $G(P_0)_{Te}$ and $G(P_0)_{As}$ are calculated for different substrates from the main target of $As_{25}Te_{75}$. These results are shown in Table lb. The compositions of As, Te and Ge obtained from the electron micro probe analysis are listed in Table lc.

Table 1a. The calculated values of $G(P_0)_{Ge}$

Ge Slices	Substrates #1	#2	#3	#4	#5
1	3.618	2.742	2.136	0.930	0.678
2	2.884	2.937	3.065	1.031	1.006
3	1.320	1.705	2.504	2.725	2.243
4	0.274	0.409	0.781	0.589	0.495
Total	8.096	7.793	8.486	5.275	4.422

Table 1b. Normalized values of $G(P_0)_{Ge}$, $G(P_0)_{As}$ and $G(P_0)_{Te}$

Substrates	#1	#2	#3	#4	#5
$G(P_0)_{Ge}$	9.0%	7.9%	7.8%	5.3%	4.9%
$G(P_0)_{Te}$	68.3%	69.1%	69.1%	71.0%	71.3%
$G(P_0)_{As}$	22.7%	23.0%	23.1%	23.7%	23.8%

Table 1c. Atomic percentages of Ge, Te and As obtained from electron microprobe analysis

Substrates		#1	#2	#3	#4	#5	Conditions of Sputtering
	Ge	6.6	4.9	4.9	2.4	1.6	
Run #1	Te	64.3	59.9	60.5	61.6	63.5	No bias
	As	29.1	35.2	34.6	36.0	34.9	

Table 1c. Continued

Substrates		#1	#2	#3	#4	#5	Conditions of Sputtering
	Ge	6.8	5.4	5.9	2.3	1.6	
Run #2	Te	60.0	61.3	60.9	63.8	65.0	No bias
	As	33.2	33.3	33.2	33.9	33.4	
	Ge	9.8	8.4	7.9	4.3	3.4	
Run #3	Te	58.5	58.7	61.3	62.1	61.5	20% bias
	As	31.7	32.9	30.8	33.6	35.1	

If one assumes that the rate of deposition $R_J(0')$ is the same for all the constituents, then the deposition profiles listed in Table 1b may be roughly regarded as the calculated compositions of the different constituents. From a comparison of Table 1b (calculated compositions) and Table 1c (observed compositions) it is observed that the percentage of Te determined from microprobe analysis is less than the calculated percentage. A similar loss in Te has also been observed by Dr. B. F. T. Bolker[18] in his samples and he has explained it as the result of a poor sticking coefficient for Te. Assuming that all atoms of As and Ge leaving the target stick to the substrate, an estimate of the sticking coefficient of Te can be made in the following manner.

For substrate #3, the observed film composition is 60.5 at. % Te, 34.6 at. % As and 4.9 at. % Ge. The calculated composition is 69.1 at. % Te, 23.1 at. % As and 7.8 at. % Ge.

For every 30.9 atoms of As + Ge one expects 69.1 atoms of Te whereas one observes 47.3 atoms of Te. Thus the sticking coefficient of Te at 20° C is $\frac{47.3}{69.1} = 0.68$. Similar calculations on other substrates show that the sticking coefficient of Te lies somewhere between 0.63 to 0.73. Dr. B. F. T. Bolker[18] has reported that the sticking coefficient varies with the substrate temperature. The sticking coefficient of Te as reported by him was 0.61 at 20° C.

There is some evidence of resputtering of Te and As with 20% bias (Table 1c). This effect has also been reported by Dr. B. F. T Bolker[18] in his thesis.

B. Temperature Dependence of Resistivity

Resistance of several samples of As-Te-Ge in the form of thin films have been measured by two probe and four probe techniques. The apparatus used for the measurement was precalibrated using 100 MΩ one percent resistor in place of the thin film sample. The accuracy of the apparatus was quite good with an error of less than 3%.

All measurements were made in vacuo and in the absence of visible light. No electric field dependence of the conductivity was detected over the range of fields employed [0.6 v/cm to 6 v/cm]. The thickness as well as the resistances by the two probe and four probe methods (Fig. 9) are shown in Table 2 for four samples at room temperature (300 K). There is fairly good agreement in the resistivity values measured by the two probe and four probe methods. This result suggests that the films are homogeneous and the resistance of the contact electrodes is negligible.

Table 2. Two probe and four probe resistances at room temperature

Sample	Thickness (Å)	Resistance (MΩ)		Resistivity (Ω-cM)	
		Two probe	Four probe	Two probe	Four probe
#12	20861	270	88	1.02×10^{4}	1.10×10^{4}
#13	28590	480	112	2.24×10^{4}	1.70×10^{4}
#14	21031	480	230	1.49×10^{4}	2.26×10^{4}
#15	13526	235	83	0.93×10^{4}	1.08×10^{4}

Table 3. Activation energy and transition temperature

Sample	Activation energy (eV)		Difference in activation energy	Transition temperature (K)
	Low temperature	High temperature		
#12	0.26	0.32	0.06	282
#13	0.29	0.45	0.16	286
#14	0.38	0.53	0.15	293
#15	0.25	0.30	0.05	276

Table 4. Composition, activation energy, energy gap (optical absorption) and σ_0

Sample	Composition			Activation energy (eV)	Energy gap (eV)	$\sigma_0(\Omega^{-1}cm^{-1})$
	As	Te	Ge			
#12	33	59	8	0.32	-	20
#13	31	61	8	0.45	0.92	300
#14	34	62	4	0.38	0.85	80
#15	35	62	3	0.30	0.76	10

A kink has been observed in the plot of resistivity versus $10^3/T$ in all samples (Fig. 8). The activation energies in the high and low temperature regions and the transition temperature (where kink occurs) are listed in Table 3. The results show that the transition temperature shifts towards higher temperature with an increase in the activation energy.

The activation energy, energy gap (optical absorption data), and σ_0 (σ at $\frac{1}{T} = 0$) are listed in Table 3 together with the composition for all four samples. The values of σ_0 have been determined from the extrapolation plots of $\log_{10}\sigma$ against $10^3/T$ (Fig. 10). The value of σ_0 lie in the range 10 $\Omega^{-1}cm^{-1}$ to 300 $\Omega^{-1}cm^{-1}$.

C. Sample Thickness Measurements

In order to measure the thickness of the thin film samples they were first coated with silver in an evaporation chamber to a thickness of a few thousand angstroms. In an Å-scope Multiple Beam Interferometer fringes were observed. From the fringe spacing and off-set spacing at the edge of the film, the thickness was determined. The Å-scope Multiple Beam Interferometer provides an absolute measure of microscope vertical surface variations in the range from 30 to 20,000 Å. Accuracy is normally ± 10 Å. The thicknesses of four different samples are given in Table 2.

D. Optical Measurements

The data on optical absorption spectra was taken by a Recording Spectrophotometer which is designed for automatic recording of

absorption spectra in the wavelength region of 1860 Å-26000 Å with good resolving power and high photometric accuracy. As shown in Table 4 the energy gaps deduced from this data (Fig. 11) are in good agreement with the activation energies ($E_\sigma = E_g/2$) determined from dc conductivity data.

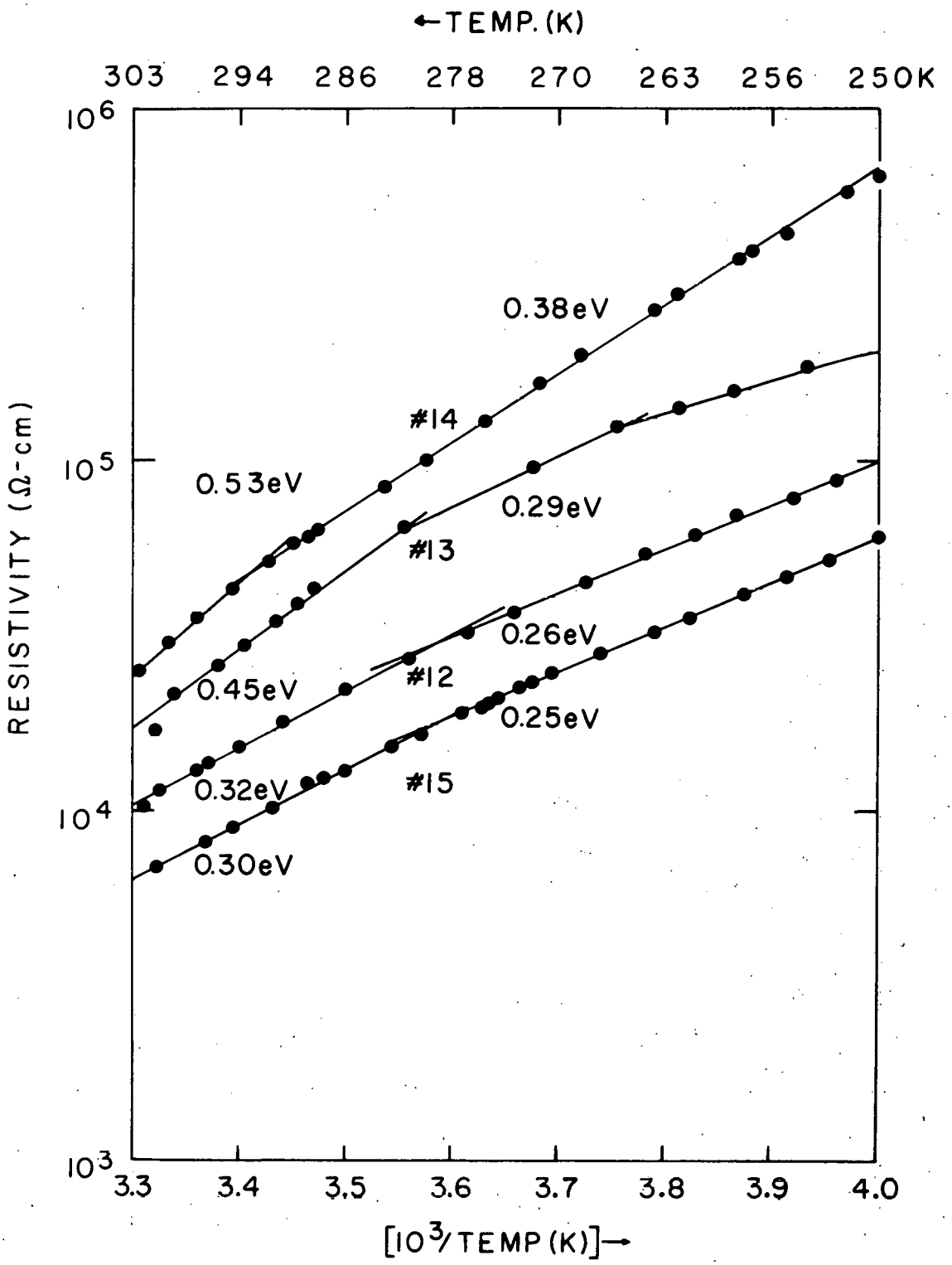

Fig. 8. Resistivity versus 10^3/temperature (K). The activation energies in the high and low temperature regions are also shown.

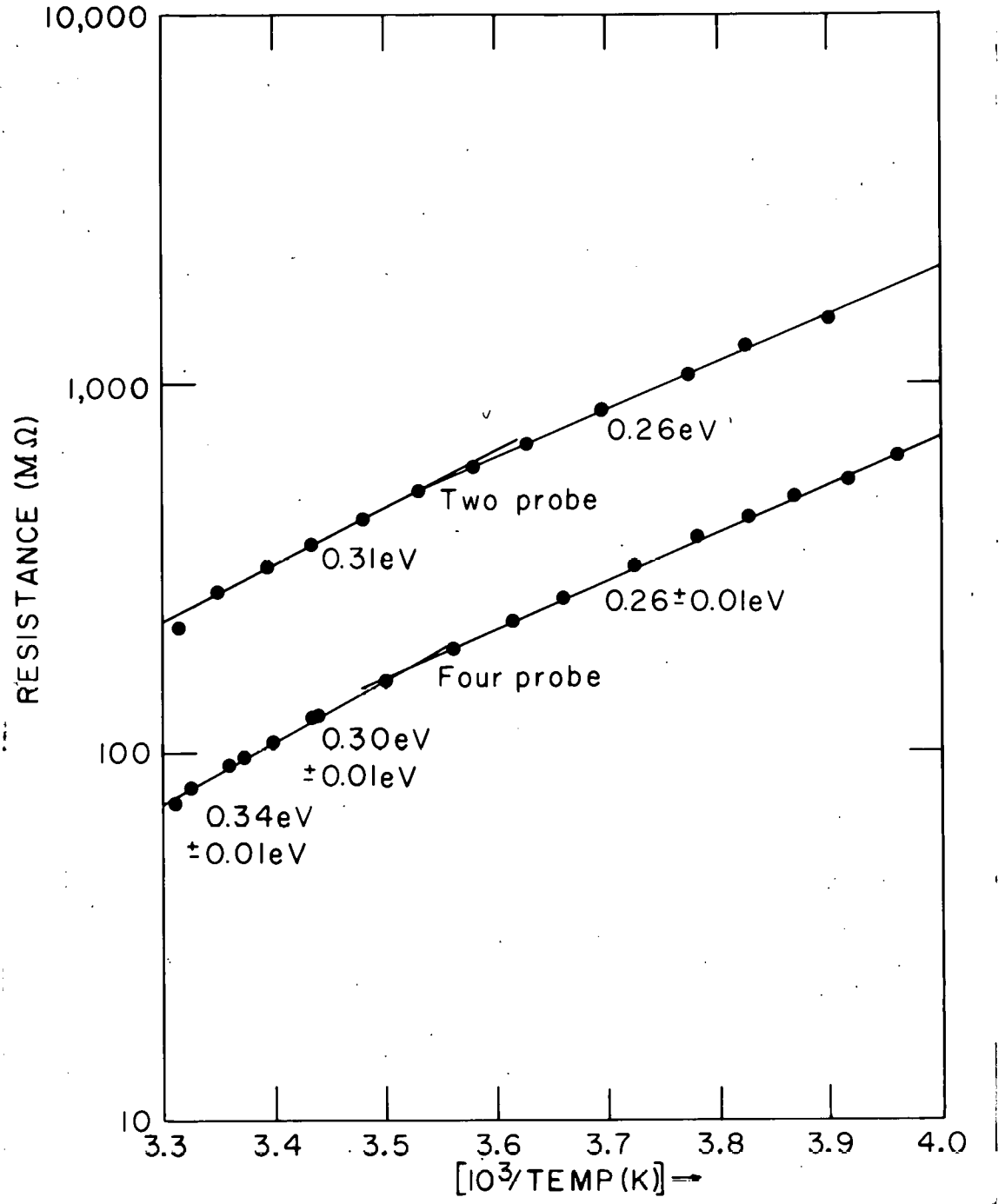

Fig. 9. Two probe and four probe measurements. The activation energies in the high and low temperature regions are also shown.

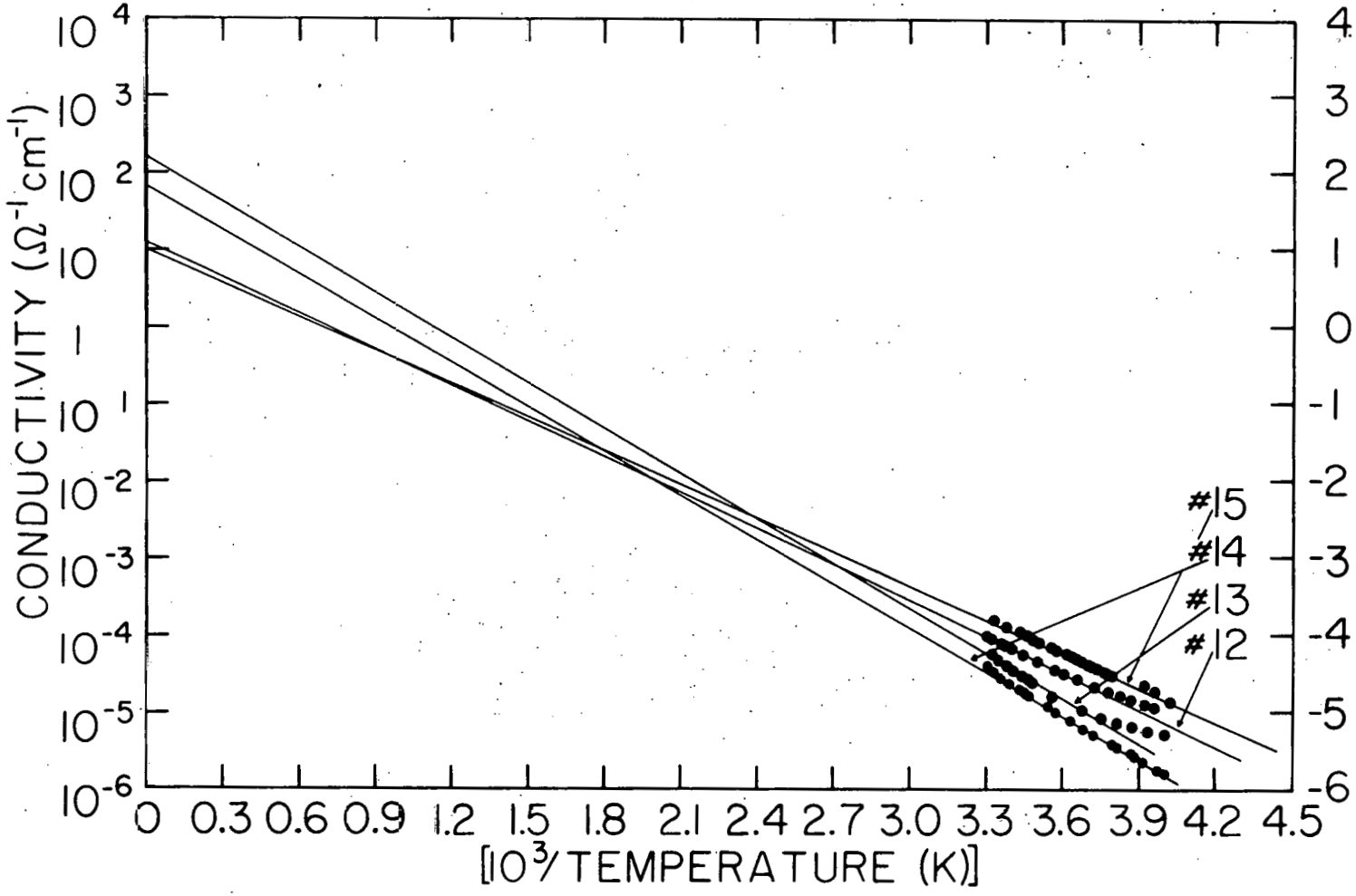

Fig. 10. Conductivity versus 10^3/temperature (K). The lines are extrapolated to determine σ_0 (σ at $1/T = 0$).

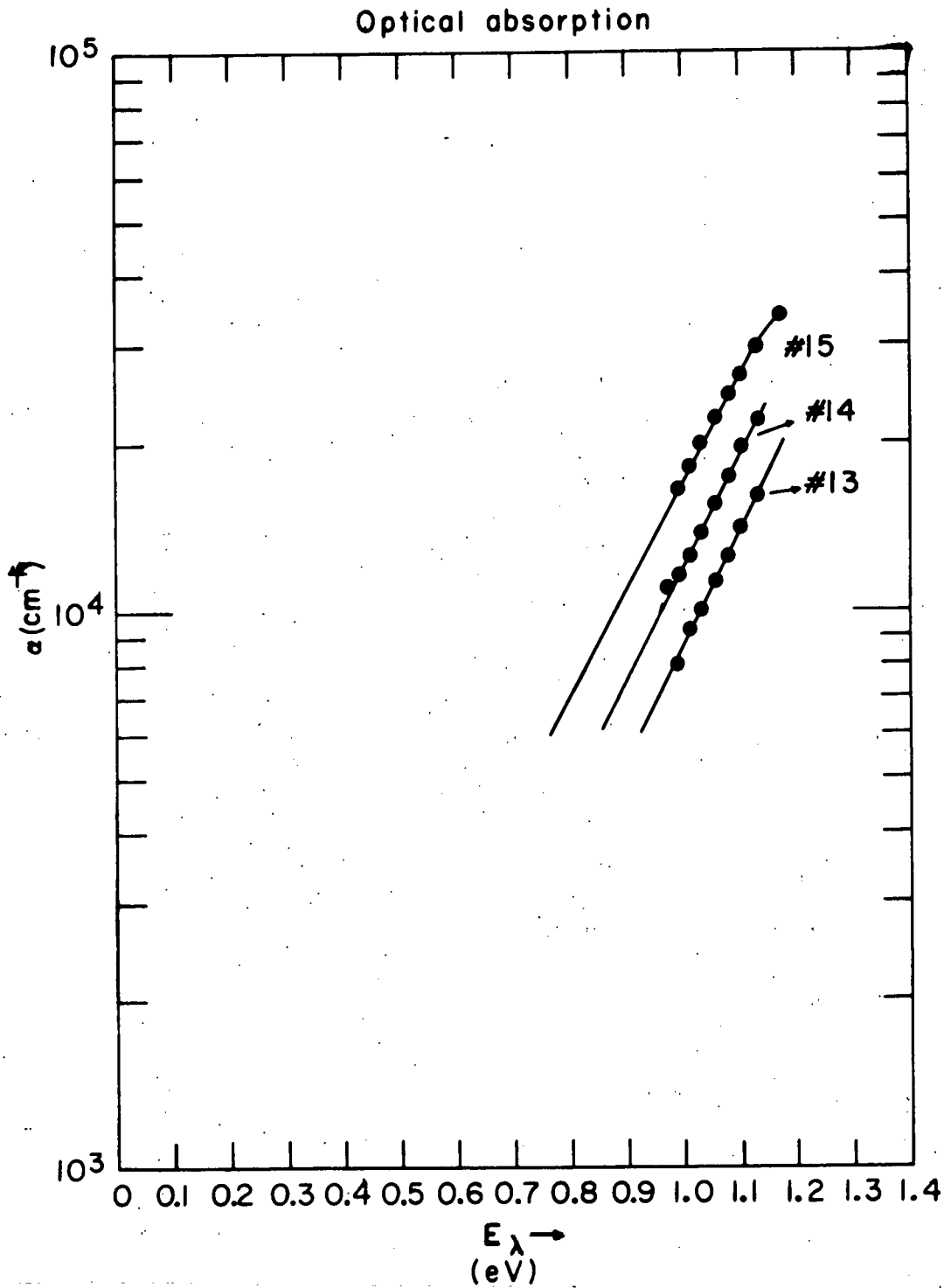

Fig. 11. Absorption coefficient α (cm^{-1}) versus photon energy E_λ(eV). The optical gaps are determined from the lower edges of the lines.

V. DISCUSSION

A. Temperature Dependence of Conductivity

Three mechanisms of electrical conduction in amorphous semiconductors have been suggested by Mott and Davis.[8] The model of energy bands predicted by them is shown in Fig. 12a. The mobility edges for electrons and holes lie at E_c and E_v. The first kind of localized states extend only to E_A and E_B in the mobility gap, and are supposed to originate from lack of long range order. The second kind of localized states near the Fermi level are assumed to arise from defects in the structure. The defect states form longer tails but are in sufficient in density to pin the Fermi level. According to this model, total conductivity will vary with temperature as shown in Fig. 12b.

(1) At high temperatures the conduction is due to carriers excited beyond the mobility shoulders into the extended states (non-localized states).

(2) At low temperatures conduction is due to carriers excited into the localized states at the band edges (E_A or E_B).

(3) At very low temperatures the conduction is due to carriers hopping between localized states near the Fermi energy. In region (1) if the main current is carried by holes

$$\sigma = \sigma_0 \exp \{ - \frac{(E_F - E_v)}{kT} \} \qquad (5)$$

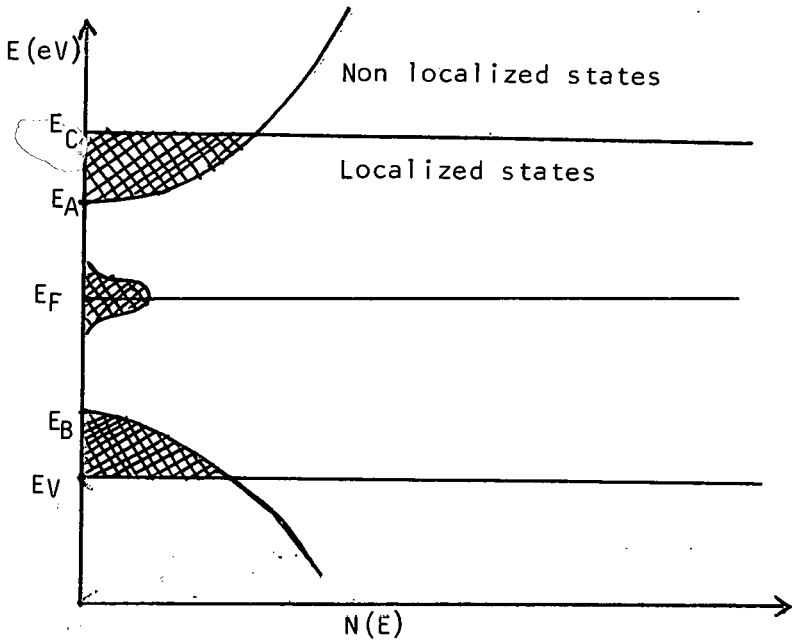

Fig.12a. Energy bands in amorphous semiconductors

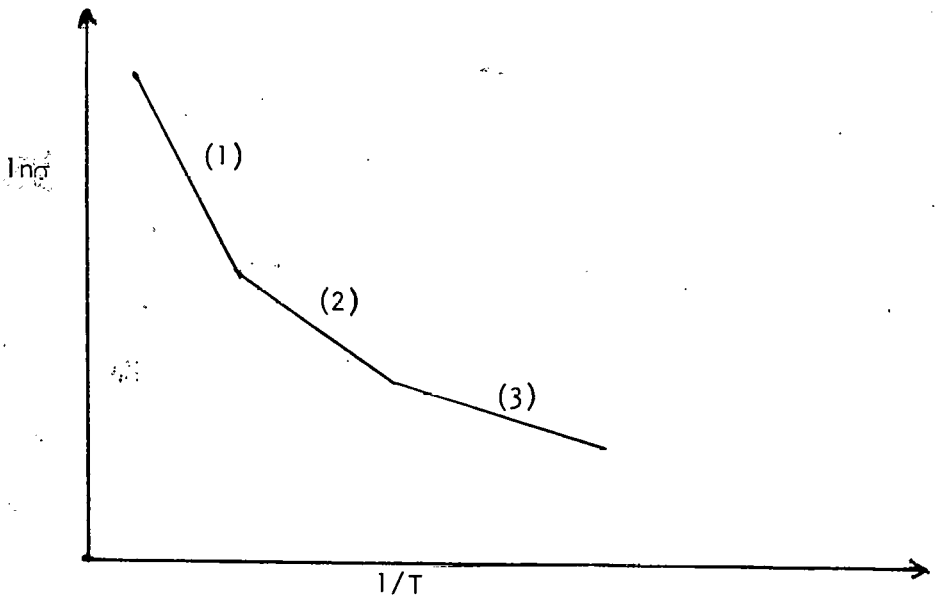

Fig.12b. Temperature dependence of conductivity

where σ_0, which is characteristic of the material, lies in the range $10^2\,\Omega^{-1}\,cm^{-1}$ to $10^4\,\Omega^{-1}\,cm^{-1}$.

A plot of ln σ against $\frac{1}{T}$ will yield a straight line with a slope equal to $-\frac{(E_F - E_V)}{k}$ or essentially $-\frac{E_\sigma}{k}$ where E_σ is called the activation energy determined from conductivity measurements.

In case the activation energy itself is a function of temperature then the following cases arise.

Case A: If $E_\sigma = E(0) - \gamma T$ . . . (6)

then the slope is $-\frac{E(0)}{k}$ but the intercept on the σ axis at $\frac{1}{T} = 0$ is $\sigma_0 \exp(\frac{\gamma}{k})$ which will be slightly higher than σ_0.

Case B: If $E_\sigma = E(0) - \beta(kT)^2$ . . . (7)

then the apparent activation energy Δ is

$$\Delta = -\frac{d(\ln \sigma)}{d(1/kT)} = E(0) + \beta(kT)^2 \ldots \quad (8)$$

Hence a plot of ln σ against $\frac{1}{T}$ is not a straight line but a slowly varying curve as observed in one of my samples [#13, Fig. 8].

In region (2) the conductivity can be expressed by

$$\sigma = \sigma_1 \exp\{-(E_F - E_B + \Delta W_1)/kT\} \quad (9)$$

where ΔW_1 is the activation energy for hopping and E_B is the energy at the band edge. An estimate of σ_1 is rather difficult to make but it is expected to be a factor of $10^2 - 10^4$ less than σ_0, factor of approximately $\frac{(E_B - E_V)}{kT}$, but mainly due to a lower mobility. In my

results samples #12 and #13 have σ_0 values 20 Ω^{-1} cm^{-1} and 300 Ω^{-1} cm^{-1} respectively, whereas σ_1 values are 10^{-1} and 10^{-2} Ω^{-1} cm^{-1}. In region (3) conduction due to hopping of carriers in the localized states near the Fermi energy is expressed as

$$\sigma = \sigma_2 \exp\left(-\Delta W_2/kT\right) \qquad (10)$$

where $\sigma_2 \lesssim \sigma_1$ and ΔW_2 is the hopping energy of the order of half the width of the defect band shown in Fig. 12a.

A kink in the plot of ln σ versus $10^3/T$, which has been observed in my samples, has also been observed in amorphous silicon films at 240 K by P. G. Lecomber and W. E. Spear.[21] They also measured drift mobilities in the same temperature range and they note a shift in the activation energy of the mobility at the same temperature. Their results are reproduced in Fig. 13. Lecomber and Spear assume the band diagram (Fig. 13b) and interpret their results by saying that excess electrons drift into the extended states with a mobility of about 10 cm^2 sec^{-1} V^{-1}. At lower temperatures phonon assisted hopping occurs through localized states occupying a range of 0.2 eV below the extended states. The change in the gradient from 0.62 eV to 0.51 eV at $T_c \simeq 240$ K corresponds to a change of 0.10 eV in the activation energy of the mobility at the same temperature.

It appears that the same kind of transition in the conduction mechanism occurs in the samples (As-Te-Ge) that I have measured. As shown in Fig. 14a for sample #12 the activation energy for conductivity changes from 0.32 eV to 0.26 eV at $T_c \simeq 282$ K. This result

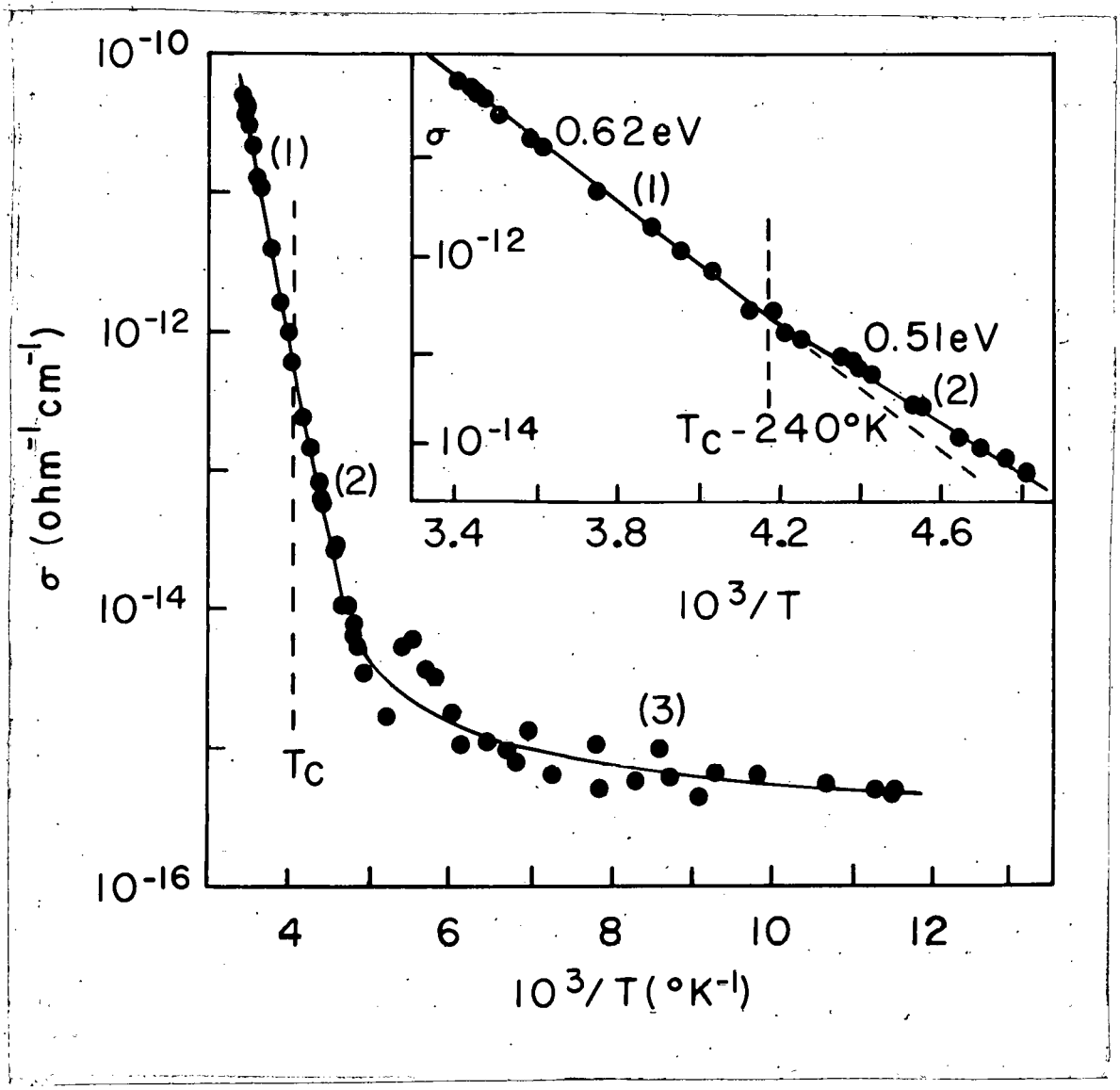

Fig. 13a. Conductivity data on amorphous silicon from Lecomber and Spear.[21] On top at the right hand corner is a magnified portion of region (1) and (2) with the corresponding activation energies.

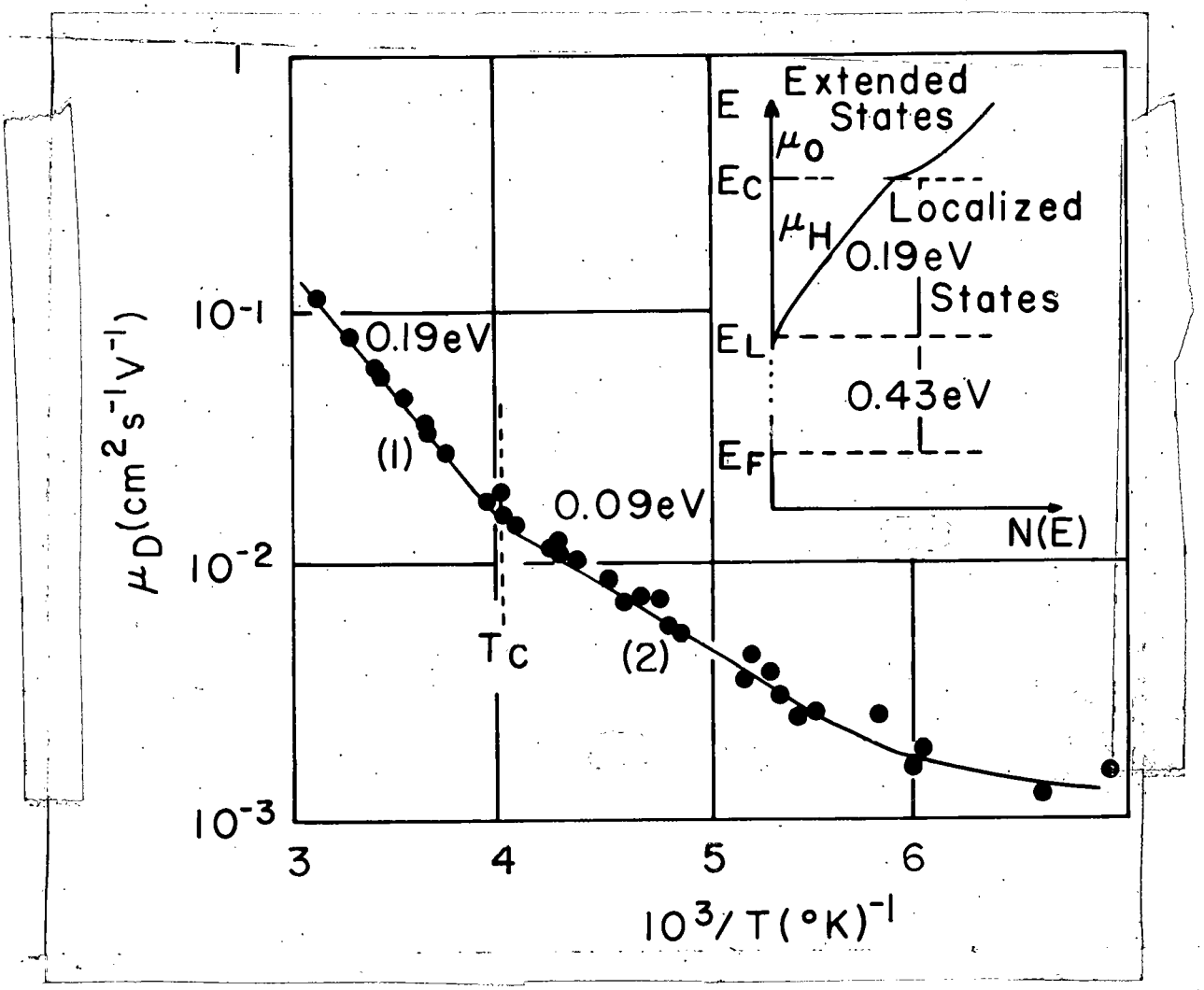

Fig. 13b. The drift mobility versus 10^3/temperature (K) for amorphous silicon from Lecomber and Spear.[21] The mobility activation energies are also shown. On top at the right hand corner is energy band diagram proposed by Lecomber and Spear.

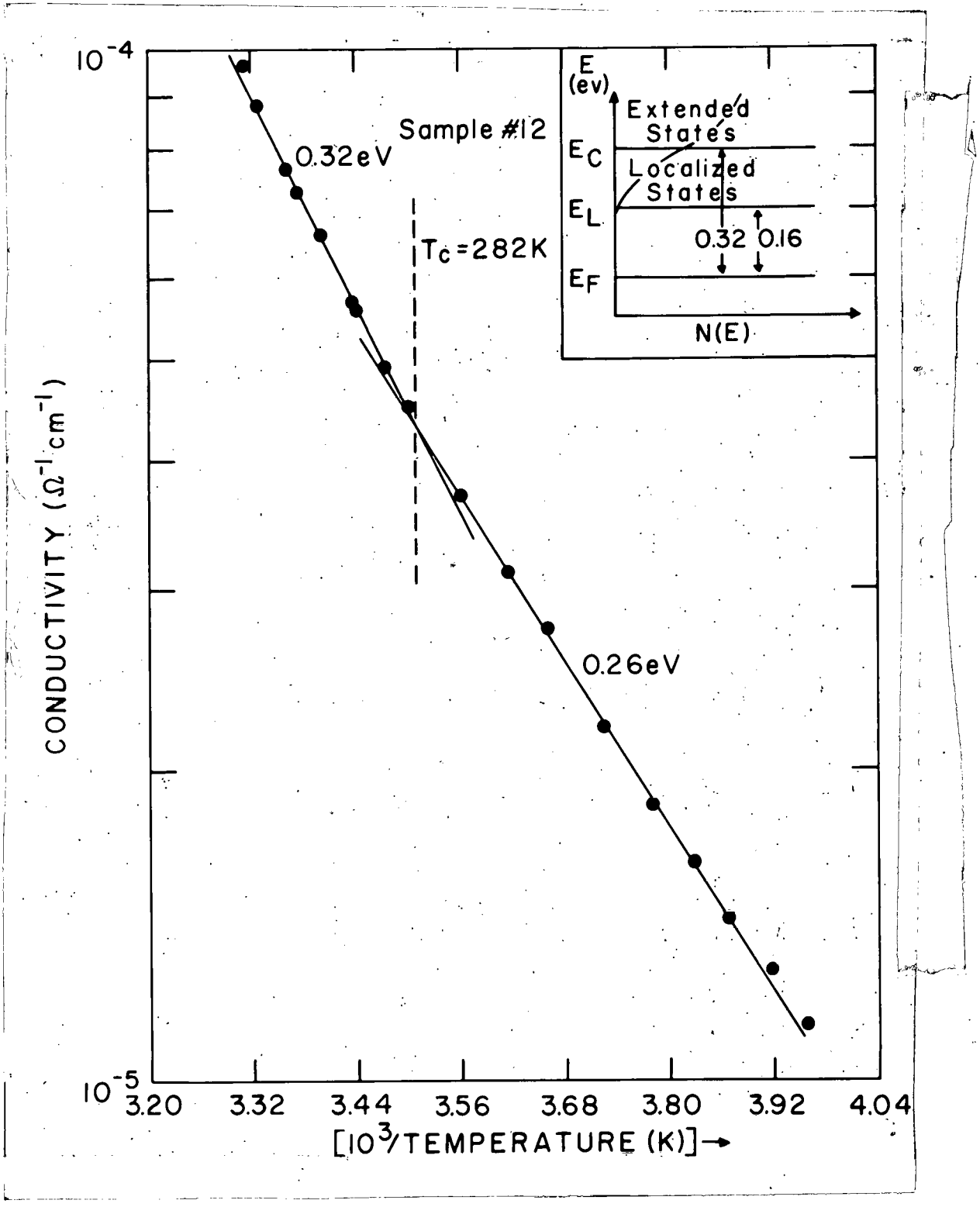

Fig. 14. Conductivity versus 10^3/temperature (K) for sample #12. The proposed energy band diagram is shown on top at the right corner.

can be explained assuming the band diagram shown in Fig. 14b. In region (1) $T > 282$ K, $E_\sigma = 0.32$ eV corresponds to intrinsic conductivity with a band gap of 0.64 eV whereas in region (2) $T < 282$ K, $E_\sigma = 0.26$ eV suggests hopping conduction in localized states with an activation energy of 0.10 eV. Hence I assume that the localized states extend 0.16 eV below the conduction band. Although the drift mobility has not been measured it is suggested that there is a corresponding change in the mobility activation energy from 0.16 eV to 0.10 eV at $T_c \simeq 282$ K.

A number of research papers indicate that the values of E_σ and σ_0 decrease with decreasing temperature as witnessed by the author in his own samples. This decrease is generally related to change in the conduction mechanism, the intrinsic conduction gradually being replaced by the hopping conduction. Eagen and Fritzsche[16] are of the opinion that thermally activated hopping conduction with an activation energy less than the mobility gap should be observed not too far below room temperature. However there are two crucial experiments that bring out the differences between band conduction and hopping conduction.[22]

(1) The dependence of conductivity on the degree of compensation is consistent with hopping but not with band conduction.

(2) The frequency dependence of a.c. conductivity should be quite different for hopping and band conduction. In hopping conduction σ increases with increasing frequency whereas in band conduction σ decreases with increasing frequency.

However, it is generally believed that hopping conductivity is negligible at room temperature. A change in conductivity at or around room temperature from intrinsic to extrinsic can sometimes be related to a structural change in the solid. Tanaka et al.[23] have measured the temperature dependence of the resistance of a bulk sample of $As_{40}Te_{50}Ge_{10}$ and they have observed a kink at the glass transition temperature ($T_g \simeq 450$ K). The glass transition temperature of the As-Te-Ge samples with the same composition as that of my samples has not been reported because it is difficult to prepare bulk amorphous samples of the same composition by quenching. In this composition range normally the samples turn out to be crystalline rather than amorphous.

But from the three dimensional figures showing the glass transition temperature of different compositions of As-Te-Ge (prepared by Mr. H. R. Shanks, one of our group members) it appears that the glass transition temperature for my samples must be substantially low. In case the glass transition temperature for these samples is at or around room temperature then it is likely that the observed kink is due to change in structure rather than change in the conduction mechanism. At this point, the question whether the kink is due to change in structure or change in the conduction mechanism is not yet resolved.

B. Resistivity and Composition

The resistivity data and data on E_σ for different compositions of As-Te-Ge by several research workers are compared with my data by

plotting resistivity and E_σ versus percentage of Ge in Fig. 15a and Fig. 15b respectively. The values of resistivity at room temperature obtained by me fit very well with the values of other workers. There is a tendency of increasing resistivity with an increase in the percentage of Ge. Referring to Table 5 it appears that with an increase in Ge-Ge bonds there should be a decrease in the number of conduction electrons because it takes much more energy to break a Ge-Gc bond compared to an As-As or a Te-Te bond.

Table 5. Bond energies in Te-As-Ge system.[18]

Bond	Energy (kJ/mole)
Ge-Ge	188
Ge-As	187
As-As	180
Ge-Te	156
As-Te	152
Te-Te	123

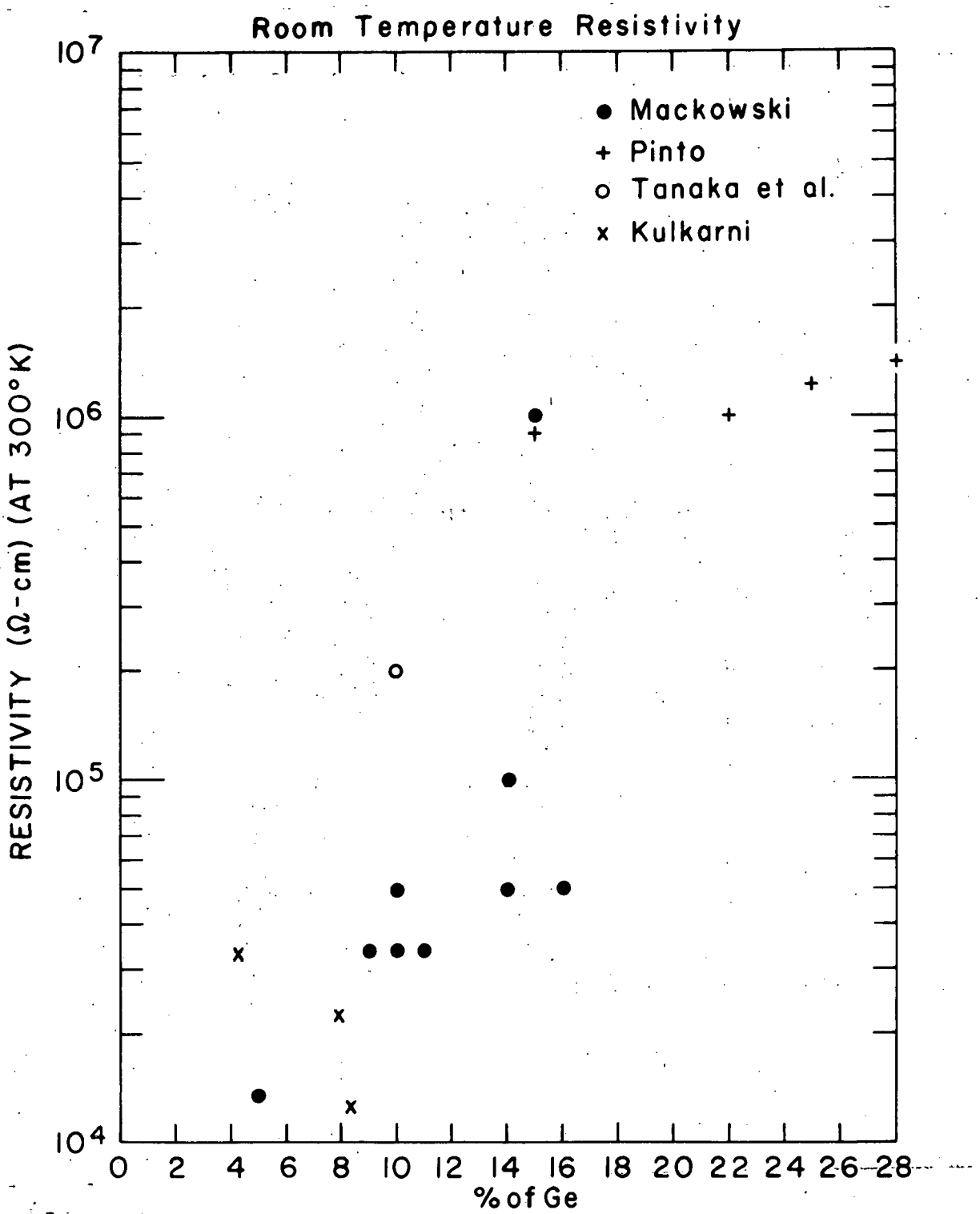

Fig. 15a. Resistivity (at 300 K) versus percentage of Ge. The symbols correspond to the authors listed on top at the right hand corner.

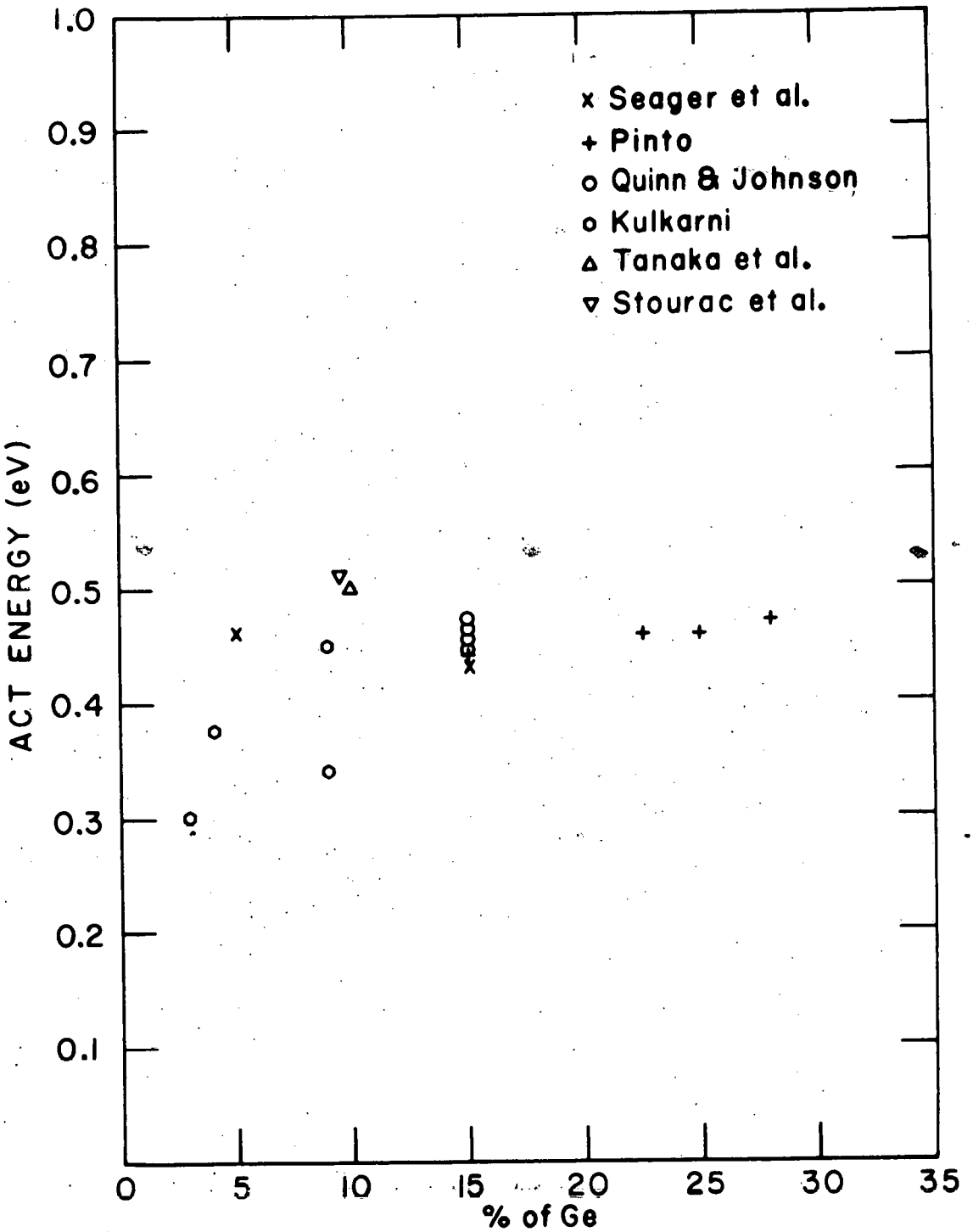

Fig. 15b. Conductivity activation energy versus percentage of Ge. The symbols correspond to the authors listed on top at the right hand corner.

VI. SUMMARY

This investigation of temperature dependence of resistivity of thin film samples of chalcogenide glasses (As-Te-Ge) has demonstrated that the values of activation energy and σ_0 for these samples obtained from RF sputtering lie close to the values of activation energy and σ_0 for bulk and evaporated samples. Two possible models have been suggested to explain the sharp change in activation energy at 285 ± 10 K. One may interpret the kink (change in slope) in the plot of resistivity versus $10^3/T$ as the result of a change in the conduction mechanism from band conduction to hopping conduction. Alternatively, one may interpret the change in slope as the result of a slight change in structure at the glass transition. The question whether the kink is due to a change in the conduction mechanism or a change in the structure is not yet resolved.

In order to reach a definite conclusion one might observe x-ray diffraction patterns of my samples at different temperatures. It is a well-known fact that the characteristic peaks observed in the x-ray diffraction pattern of crystalline solids are not observed in the case of an amorphous solid. It is believed that a change in the structure, if it exists, should somehow manifest itself in x-ray diffraction patterns observed at different temperatures.

VII. LITERATURE CITED

1. S. R. Ovshinsky, Phys. Rev. Letters 21, 1450 (1968)
2. H. K. Henisch, Sci. Amer. 30 (Nov. 1969)
3. G. Lapidus, IEEE Spectm. 44 (Jan. 1973)
4. B. T. Kolomiets and T. F. Nazarova, Sov. Phys. Solid State 2, 369 (1960)
5. A. R. Hilton, C. E. Jones, R. D. Dobrott, H. M. Klein, A. M. Bryant and T. D. George, Phys. and Chem. of Glasses 7, 116 (1966)
6. S. D. Senturia, C. R. Hewes and D. Adler, J. Appl. Phys. 41, 430 (1970)
7. D. Adler, "Amorphous Semiconductors" CRC Press (1971)
8. N. F. Mott and E. A. Davis, "Electronic Processes in Non-crystalline Materials" Clarendon, Oxford (1971)
9. R. K. Quinn and R. D. Johnson, Jr., J. Non-crystalline Solids 12, 213 (1973)
10. J. M. Mackowski, J. J. Samueli, P. Kumurdjian and G. Bourdavios. J. Non-crystalline Solids 8-10, 985 (1972)
11. R. Pinto, J. Non-crystalline Solids 6, 187 (1971)
12. G. V. Bunton, S. C. M. Day, R. M. Quilliam and P. H. Wisbey, J. Non-crystalline Solids 6, 251 (1971)
13. C. H. Seager, D. Emin and R. K. Quinn, Phys. Rev. B 8, No. 10, 4746 (1973)
14. V. R. Panus, Ya. M. Ksendzov and Z. U. Borisova, Neorg. Mat. 4, 885 (1968)
15. H. K. Rockstad, J. Non-drystalline Solids, 2, 192 (1970)

16. E. A. Fagen and H. Fritzsche, J. Non-crystalline Solids 2, 180 (1970)

17. R. L. Johnson, M. S. Thesis, Iowa State University, Ames, Iowa (1966)

18. B. F. T. Bolker, Ph.D. Thesis, Iowa State University, Ames, Iowa (1975)

19. J. W. Colby, Paper 17 of 6th National Conference on Electron Probe Analysis, Pittsburgh, PA (1971)

20. J. J. Hanak, H. W. Lehmann and R. K. Wehner, J. Appl. Phys. 43, 1666 (1972)

21. P. G. Lecomber and W. E. Spear, Phys. Rev. Lett. 25, 509 (1970)

22. F. J. Blatt, "Physics of Electronic Conduction in Solids," McGraw-Hill, New York (1968)

23. K. Tanaka, Y. Okada, M. Sugi, S. Iizima and M. Kikuchi, J. Non-crystalline Solids 12, 100 (1973)

VIII. ACKNOWLEDGMENTS

I wish to express my sincere thanks to Dr. G. C. Danielson for his guidance and encouragement during this research. The valuable assistance of Dr. B. F. T. Bolker and Mr. Jim Andregg in the preparation of the samples and sample holder is highly appreciated. I am grateful to Mr. O. M. Sevde for his timely technical help. Mr. F. Laabs performed the electron microprobe analysis of my samples and Dr. Lynch helped me take optical absorption data. I owe special thanks to both of them. Mr. Charles Culp and Mr. H. R. Shanks also deserve my thanks for their helpful discussions.

Finally I thank my wife Vasu for her unselfish love and cooperation throughout this investigation.